


Cite this: *RSC Adv.*, 2024, 14, 28376

Zn–Al and Mg–Al layered double hydroxide nanoparticles improved primary and secondary metabolism of geranium plants†

Shimaa Hashem,^{‡*a} Hamada AbdElgawad,^{‡b} Fatma Mohamed,^{cde} Momtaz M. Hegab,^a Amal Mohamed AlGarawi,^{id f} Mohammad K. Okla^f and Mona Sayed^{id a}

Layer double hydroxide (LDH) nanoparticles (NPs) have been applied to enhance plant growth and productivity. However, their effects on carbon and nitrogen metabolism of aromatic plants, are not well understood. Therefore, we investigated the impact of foliar application of Zn–Al LDH and Mg–Al LDH NPs (10 ppm) on the growth and metabolism of geranium plants. Zn–Al LDH and Mg–Al LDH NPs significantly increased the dry biomass, photosynthetic pigment, and Zn and Mg uptake by treated plants. These increases were consistent with increased primary metabolism such as soluble sugars and their metabolic enzymes (invertase and amylase). The supply of high sugar levels induced TCA organic accumulation, providing a pathway for amino acid biosynthesis. Among amino acids, proline level and its biosynthetic enzymes such as pyrroline-5-carboxylate reductase (P5CR), ornithine aminotransferase (OAT), and pyrroline-5-carboxylate synthetase (P5CS), glutamine synthetase (GS), and arginase were increased. Increased primary metabolites can then be channeled into secondary metabolic pathways, leading to higher levels of secondary metabolites including tocopherols, phenolics, and flavonoids. These observed increases in primary and secondary metabolites also improve the biological value of geranium plants. Overall, our research highlights the potential of Zn–Al LDH and Mg–Al LDH NPs as elicitors to enhance metabolism in geranium plants, thereby improving their growth bioactivity.

Received 11th June 2024
Accepted 24th August 2024

DOI: 10.1039/d4ra04280h

rsc.li/rsc-advances

1. Introduction

Nanotechnology is a modern research field dealing with materials having a particle size of less than 100 nm, with diverse applications in various fields.¹ Nanotechnology has become a crucial field in modern agriculture, facilitating accelerated plant growth and offering improved plant protection with less environmental impact compared to traditional approaches.² The use of layered double hydroxide (LDH) nanoparticles (NPs)

in agriculture influences plants' physiological and biochemical processes by fertilizing and suppressing pests.³ The physico-chemical properties of NPs include a high surface-to-volume ratio.⁴ These features enable the use of NPs as fertilizers, which aids plant growth and development by allowing for the targeted and regulated release of mineral nutrients.⁵

LDHs are a type of ion exchanger with alternating positively charged metal hydroxide layers and negatively charged inter-layer anions.⁵ LDH NPs are considered environmentally safe.⁶ They also possess a unique layered structure that enables ion exchange, resulting in more effective slow-release fertilizers for nutrients.^{5,7} Furthermore, the advantages of LDH NPs over other NP alternatives are their low toxicity, regulated release, and biocompatibility.⁸ Zinc–aluminum (Zn–Al) LDH and magnesium–aluminum (Mg–Al) LDH have attracted a lot of attention due to their unique properties compared to other nanomaterials. Zn–Al LDH consists of alternating Zn²⁺ and Al³⁺ layers with hydroxide ions (OH[−]) in between, while Mg–Al LDH consists of alternating Mg²⁺ and Al³⁺ layers with hydroxide ions (OH[−]) in between. In agreement, previous studies showed that Zn²⁺ and Mg²⁺ ions incorporated into LDH structures can form Zn(OH)₂, ZnO, Mg(OH)₂, and MgO. Zn–Al and Mg–Al LDH NPs have excellent biocompatibility and bioavailability, making them suitable for agricultural use. Their controlled release

^aBotany and Microbiology Department, Faculty of Science, Beni-Suef University, Egypt.
E-mail: ShimaaHashem@science.bsu.edu.eg

^bIntegrated Molecular Plant Physiology Research, Department of Biology, University of Antwerp, Antwerpen, Belgium

^cChemistry Department, Faculty of Science, Beni-Suef University, Beni-Suef 62514, Egypt

^dNanophotonic and Applications (NPA) Lab, Faculty of Science, Beni-Suef University, Beni-Suef 62514, Egypt

^eMaterials Science Research Lab, Chemistry Department, Faculty of Science, Beni-Suef University, Beni-Suef 62514, Egypt

^fBotany and Microbiology Department, College of Science, King Saud University, PO Box 2455, Riyadh 11451, Saudi Arabia

† Electronic supplementary information (ESI) available. See DOI: <https://doi.org/10.1039/d4ra04280h>

‡ Authors are equal contribution.



properties minimize toxicity risks and ensure essential nutrients are available to plants. When they are applied at appropriate concentrations, they enhance nutrient uptake and promote plant growth without inducing toxicity.⁹ LDHs combined with NPK fertilizers effectively promote plant growth and reduce nutrient leaching in soil.^{10–12} In addition to agriculture applications, their *in vivo* and *in vitro* biocompatibility is utilized for gene delivery, drug delivery, bioimaging, and bio-sensing areas.¹³ Zn–Al and Mg–Al LDH improve the bioavailability of essential nutrients by providing a steady and controlled release of ions such as Zn^{2+} and Mg^{2+} .^{5,7}

Many metabolic functions in plants rely on Zn and Mg.¹⁴ Zn is an essential mineral element required for several physiological activities, including the formation of carbohydrates, proteins, and chlorophyll.^{15,16} Mg is a crucial component of chlorophyll because it is the center atom and keeps ribosomes structurally intact, which is necessary for protein synthesis, and also activates several enzymes.¹⁷ Fertilizers containing Zn and Mg have a beneficial effect on mineral absorption and cell division, which increases plant growth.¹⁸ Numerous NPs have a major impact on the growth and development of plants, as recent studies have shown. For instance, it has been shown that applying ZnO NPs significantly enhanced the growth of wheat, maize, and cotton, increasing crop production.^{19–21} Similarly, macronutrient levels in cotton plants, such as nitrogen (N), phosphorus (P), potassium (K), and Mg, were significantly and favorably affected by the foliar application of MgO NPs. In this context, a dose of 60 ppm of MgO NPs was found to be the optimal dose for increasing the SPAD chlorophyll value, which resulted in increased cotton growth.²² Tobacco plants treated with MgO NPs exhibit higher Mg absorption and growth stimulation.²³

NPs not only affect primary growth parameters but also play a crucial role in modulating metabolic pathways. NPs increase sugar accumulation, indicating the availability of carbon for the biosynthesis of both primary and secondary metabolites.²⁴ The impact of NPs has a significant effect on related metabolic pathways, such as the sugar and proline metabolism.²⁵ Sugars and proline are involved in the storage and transfer of energy.^{26–28} Thus previous research indicated that increased proline levels improved plant growth.²⁹ NPs are further supported by the upregulation of secondary metabolites, including tocopherol, phenolics, and flavonoids.³⁰ These secondary metabolites are typically present in low concentrations and play a crucial role in all living organisms as antioxidants.³¹ Overall, there has been an increasing interest in these substances due to their practical applications in nutrition, medicine, and cosmetics, as well as their undeniable role in plant stress physiology.³¹

Given the potential of LDH NPs to enhance sustainable agriculture by improving crop quality and yield, this study aims to examine the effects of Zn–Al LDH and Mg–Al LDH NPs on both the primary and secondary metabolic parameters in geranium plants. We specifically investigated their effects on growth (shoot fresh weight and shoot dry weight), photosynthesis, primary metabolism, and the production of secondary metabolites such as flavonoids, phenolics, and tocopherols. Our goal is to gain a comprehensive understanding of the potential benefits of LDH NPs in enhancing geranium growth by elucidating these effects.

2. Materials and methods

2.1. LDH NP synthesis and characterization

The co-precipitation techniques were utilized to synthesize Mg–Al and Zn–Al LDH.^{32–34} Mg–Al LDH and Zn–Al LDH (molar ratio of 2 : 1) were synthesized using the co-precipitation method. MgSO_4 (0.2 M) and $\text{Al}_2(\text{SO}_4)_3$ (0.1 M) were dissolved in 100 mL H_2O , and the pH was adjusted to 10 using 2 N NaOH under vigorous stirring at 60 °C. After 24 hours of stirring, the prepared LDH was collected and washed several times with warm distilled water until the pH reached 7 and then dried at 50 °C overnight.^{32–34} To prepare 10 ppm of Mg–Al and Zn–Al LDH, 10 mg of catalyst was dissolved in 1000 mL of distilled water under continuous stirring for 3 hours. In parallel, Zn–Al LDH was synthesized using zinc sulfate (0.2 M). Stabilization of Zn–Al LDH and Mg–Al LDH NPs was measured through zeta potential analysis. All emulsions exhibited zeta potential values exceeding -30 mV, suggesting the presence of enough repulsive force between particles, ensuring colloidal stability. The samples of ZnAl LDH and MgAl LDH were found to have negative charges of -35.7 mV and -36.3 mV, respectively. The zeta potential experiments were conducted to assess the stability and charge of the NPs, based on their electrophoretic mobility.³⁵

The ZS Malvern Zetasizer, using DLS and an automatic titrator, measured the particle size distribution, showing polydispersity with peaks at 2903 nm and 892 nm and average PDI of 0.6 and 0.1 for ZnAl LDH and MgAl LDH, respectively (Fig. 2). These sizes are larger than those from SEM and XRD (ESI Fig. 1 and 2†) due to NP aggregation in the aqueous solution during DLS measurement, which doesn't occur in the dry state for SEM or XRD. The hydrodynamic diameters indicate swelling over time, reflecting the layered structure and thermal stability of LDHs in polymer matrices.

The surface properties were assessed using scanning electron microscopy (SEM). The samples were scanned in powder form, and surface modifications were done by mounting fine grains on conductive copper double-face tape, coating by gold using DC sputtering coater (SPI-instruments- Japan), and observation under Tungsten filament scanning electron microscope (ZEISS Sigma 500 VP microscope).

The crystalline structure of the synthesized materials was assessed through X-ray diffraction (XRD) analysis, using an X-ray diffractometer (PANalytical, Empyrean, Netherlands) with Cu-K α radiation (wavelength 1.54045 Å). The XRD was operated at 40 kV and a current of 30 mA. To identify various functional groups, Fourier transform infrared (FTIR) spectra of the samples were recorded using a Vertex 70 system (400–4000 cm^{-1}). Potassium bromide (KBr) was used as a control spectrum for FTIR because it is inactive in IR spectroscopy.

2.2. Experimental setup, sample collection, and treatments

The experiment was carried out in a greenhouse at Riyadh Village, located in the Beni-Suef Governorate of Egypt. The temperatures were 26 °C/18 °C Day/night, the light/dark cycle was 16/8 h, and humidity levels ranged from 50% to 60%. Clay

soil rich with nutrients was used. The soil initially contained 13.7 mg organic carbon (C), 14.8 mg nitrate-nitrogen (N), 1.1 mg ammonium-N, and 10.7 mg phosphorus (P)/g air-dry soil at a humidity of 0.33 g water/g dry soil. The pH was 7.26, EC was 3.74 dS m⁻¹ and K was 2.45 meq L⁻¹. Geranium seedlings were provided from local farmland and treated with Zn-AL LDH and Mg-Al LDH NPs. At the vegetative stage, the plants were sprayed with 10 ppm of Zn-AL LDH and Mg-Al LDH NPs. The control group was sprayed with water. After 30 days of foliar application of LDH NPs, plant samples were collected for analysis. The samples' fresh weight was determined, followed by oven-drying at 70 °C. The outcomes represent the dry weights of the shoots.

2.3. Photosynthetic pigment

Total chlorophyll was measured using 80% acetone to extract 0.5 gm of fresh leaves, followed by centrifugation (10 000 g for 5 min). Results were expressed as (mg gm⁻¹ f.wt.).³⁶

2.4. Estimation of Zn and Mg content

Grounded geranium leaf (0.3 gm) was added to a digestive vessel and then mixed with 10 mL of 6 N HCl. The resulting mixture was heated on a hot plate using a thermostat set to 45 °C for 24 hours, keeping the temperature at 50 °C or below. Following digestion, the materials were put into a 25 millilitre volumetric flask and precisely diluted with deionized water. The technique of atomic absorption spectrophotometry (AAS) was used to quantify the amounts of zinc and magnesium present in the digested tissues after they had been filtered.³⁷

2.5. Measurement of soluble sugars and starch content

Soluble sugars and starch content were measured.³⁸ Sugars were extracted in 80% ethanol at room temperature. After drying, the extracts were again suspended in dH₂O. For additional analysis, the supernatants were kept in storage at -20 °C. For starch extraction, was boiled to break down the starch grains and homogenized in water. After adding one milliliter of amyloglucosidase solution (0.5 units per mL in acetate buffer pH 4.5), the mixture was shaken at 55 °C to facilitate the digestion of starch. For ten minutes, the extraction was centrifuged at 2000 g. HPLC equipped with A diode array detector was used to detect soluble sugars, and the Coulter PACE system 5500 was used to determine concentrations.

2.6. Extraction and evaluation of the major enzymes involved in sugar metabolism

Sugar metabolism enzymes were initially extracted,³⁹ and invertase activity was assessed in a TAE buffer (pH 8.5) with 0.1 M sucrose as substrate. Starch synthase activity was evaluated by using a reaction buffer containing citrate and glycogen.⁴⁰ By tracking the breakdown of starch at 620 nm, amylase enzyme activity was determined.⁴¹

2.7. Organic acids in the tricarboxylic acid cycle (TCA)

The geranium shoots were treated with a solution containing 0.1% phosphoric acid and 0.3% butylated hydroxyanisole to

extract organic acids using a MagNALyser (Roche, Vilvoorde, Belgium). The quantities of TCA organic acids were measured using an HPLC equipped with a SUPELCOGEL C-610H column and an ultraviolet (UV) detection system that operated at 210 nm (LaChrom L-7455 diode array, LaChrom, Tokyo, Japan). The mobile phase, 0.1% phosphoric acid, was eluted at a rate of 0.45 mL min⁻¹.³⁸

2.8. Metabolites of amino acids

Amino acids were extracted from geranium shoots using 80% (v/v) from aqueous ethanol. During the extraction process, norvaline—the internal standard—was introduced. The next step was centrifugation (16 000 g, 20 min). The supernatant was evaporated, and the residue was resuspended in chloroform. After centrifugation, the plant residue was extracted once more in HPLC-quality water, and the resulting supernatant was mixed with suspended chloroform pellets. The extracts were centrifuged and then run through 0.2 µm-pore size Millipore microfilters. Amino acids were separated on a BEH amide 2.1 9 50 column, and the outcomes were measured using Waters Acquity UPLC-tqd mass spectroscopy.^{42,43}

2.9. Key enzymes involved in the metabolism of amino acids: extraction and estimate

Glutamine synthetase (GS), glutamine oxoglutarate aminotransferase (GOGAT), pyrroline-5-carboxylate dehydrogenase (P5CDH), pyrroline-5-carboxylate reductase (P5CR), and pyrroline-5-carboxylate synthetase (P5CS) enzymes activities were measured.⁴⁴ The samples were extracted using Tris-HCl buffer 0.05 M (pH 7.4) containing 0.004 M DTT, 0.001 M EDTA, 10% glycerol, 2% (w/v) polyvinylpyrrolidone, 0.002 M PMSF, and 0.01 M MgCl₂. Arginase (ARG) and ornithine aminotransferase (OAT) have been extracted using 0.05 M potassium phosphate buffer (pH 7.0) containing 0.002 M PMSF, 0.01 M 2-mercaptoethanol, 0.001 M EDTA, 15% glycerol, and 2% (w/v) polyvinylpyrrolidone. Protein content in the extracts was calculated using the Lowry method.⁴⁵ Following the oxidation of NADH at A340 allowed for the measurement of P5CR activity.⁴⁶ P5CS was evaluated using the measurement of the γ-glutamyl hydroxamate synthesis at A535. After developing the reduced form of NADH at A340 nm researchers measured P5CDH activity.⁴⁷ The GOGAT activity was assessed by measuring the glutamine-dependent NADH oxidation at A340.⁴⁸ A340 produced γ-glutamyl hydroxamate, indicating the presence of GS.⁴⁹ OAT activity was measured by detecting the decrease of NADH at A340,⁵⁰ whereas ARG activity was detected by following urea accumulation with the diacetyl monoxime method.⁵¹

2.10. Tocopherol content

HPLC analysis was used to determine the tocopherols, according to the following method.⁴⁴ Using the MagNALyser (Roche, Vilvoorde, Belgium; 1 min, 7000 g), tocopherols were extracted with hexane. The tocopherols were separated and measured by HPLC (Shimadzu's Hertogenbosch, The Netherlands) (normal phase conditions, Particil Pac 5 µm column material, length 250 mm, i.d. 4.6 mm) after the dried extract (CentriVap



concentrator, Labconco, KS, United States) was resuspended in hexane. The internal standard utilized was dimethyl tocol (DMT) at 5 ppm. The software Shimadzu Class VP 6.14 was used to analyze the data.

2.11. Phenolics

Using an orbital shaker, acetone water (250 mL, 4 : 1, v/v) was used to extract geranium samples, which were left at room temperature for 24 hours. The DPF hydroxyacetone crude extract was then obtained by filtering the extracts and centrifuging them for 10 minutes at 4000 g (Hettich Zentrifugen, Tuttlingen, Germany). Using a rotary evaporator (IKA-WERKE-RV06ML, Stanfer, Germany), the supernatant was concentrated under decreased pressure for three hours at 40 °C. The residues were measured as previously stated by⁵² and dissolved in HPLC grade MeOH. A sample (20 µL) that had been dissolved in methanol was briefly injected into a Shimadzu HPLC system (SCL-10 A vp, Shimadzu Corporation, Kyoto, Japan). The HPLC system consisted of a diode-array detector and a Lichrosorb Si-60 column measuring 7 µm by 3 × 150 mm. Water/formic acid (90 : 10, v/v) and acetonitrile/water/formic acid (85 : 10 : 5, v/v/v) made up the mobile phase. The quantification of flavonoids and phenolic acids that were tentatively identified was done using a calibration curve that was obtained using the relevant standards. The findings were given as µmol gm⁻¹ DW.

2.12. Statistical analysis

All data were analyzed using one-way analysis of variance (ANOVA) followed by Duncan's multiple range test at a significance level of $P < 0.05$. Each experiment was performed at least three times ($n = 3$). SPSS version 20 was used for statistical analysis, and GraphPad Prism was used for creating the graphs. Data normality was checked by using Levene's test. PCA analysis Euclidean distance was performed using the R stat software package (version 4.5.0, the R).

3. Results

3.1. Characterization of LDH NPs

3.1.1 Scanning electron microscopy (SEM). SEM analysis revealed that Zn-Al LDH NPs appear as stacked arranged layers with non-uniform nonporous features and the average particle size is 22 nm. Mg-Al LDH NPs exhibited layer-shaped surface morphology with consistent nonporous properties and the average particle size is 41 nm Fig. S1.†

3.1.2 Fourier-transform infrared spectroscopy (FTIR). The Zn-Al LDH and Mg-Al LDH NPs' FTIR spectra showed distinctive absorption peaks, indicating the existence of crucial functional groups within the LDH structure. All LDH samples exhibited shared absorption bands, including a broad absorption band spanning the 3300–3500 cm⁻¹ range attributed to the OH stretching mode of the basal layer and interlayer water. Additionally, a band within the 1620–1650 cm⁻¹ range was credited to the bending mode of interlayer water and anion groups. A distinct band in the region of 400 to 800 cm⁻¹ was observed, related to MO and MOH vibrations. These functional groups could have significant implications for interaction with plant tissues Fig. S2.†

3.1.3 X-ray diffraction (XRD). The Zn-Al LDH and Mg-Al LDH NPs' XRD patterns confirmed the formation of crystalline phases. Zn-Al LDH NPs showed diffraction peaks at various angles, indicating a layered structure with an average crystalline size near 15–20 nm. Mg-Al LDH NPs also displayed diffraction peaks at different angles, with an average crystalline size near 30–35 nm Fig. S2.†

3.2. Growth and biomass buildup

In an experiment, we exposed geranium seedlings to Zn-Al LDH and Mg-Al LDH NPs and then measured the fresh and dry weights of the seedlings to assess their growth. Compared to the control group, the application of Zn-Al LDH and Mg-Al LDH NPs led to a significant increase in fresh weight by 34% and 39%, respectively, and dry weight by 48% and 54%, respectively Table 1.

3.3. Pigments analysis

We assessed the levels of total chlorophyll in geranium seedlings after exposing them to Zn-Al LDH and Mg-Al LDH NPs. The results in Table 1 reveal that Mg-Al LDH NPs had a favorable effect on geranium total chlorophyll. Geranium treated with Mg-Al LDH NPs had a greater total chlorophyll content (41%). Zn-Al LDH NPs demonstrated a non-significant increase in total chlorophyll.

3.4. Carbohydrates and sugar metabolism

Under Zn-Al LDH and Mg-Al LDH NPs, the amounts of soluble sugars (glucose, fructose, and sucrose) and insoluble sugars (starch) and the associated enzymes were measured in geranium Fig. 1. Obtained data showed that Mg-Al LDH NP

Table 1 The effects of Zn-Al LDH and Mg-Al LDH NPs on geranium shoot fresh weight, dry weight, total chlorophyll, and mineral content. The values show the three independent replicates' mean ± standard error. Statistically significant treatment differences ($P < 0.05$) are indicated by different letters after the means

Parameters	Control	Zn-Al LDH NPs	Mg-Al LDH NPs
Shoot fresh weight (gm)	16.9 ± 0.52b	24.9 ± 1.5a	26 ± 0.57a
Shoot dry weight (gm)	3.63 ± 0.29b	5.66 ± 0.53a	6.46 ± 0.53a
Total chlorophyll (mg g ⁻¹ FW)	8.88 ± 2.11b	10.92 ± 0.5 ab	12.59 ± 0.89a
Zn content (mg kg ⁻¹ FW)	2.6 ± 1.33c	16.9 ± 3.42a	4.1 ± 1.05b
Mg content (mg kg ⁻¹ FW)	1.33 ± 0.44c	2.4 ± 1.91b	20.2 ± 7.75a

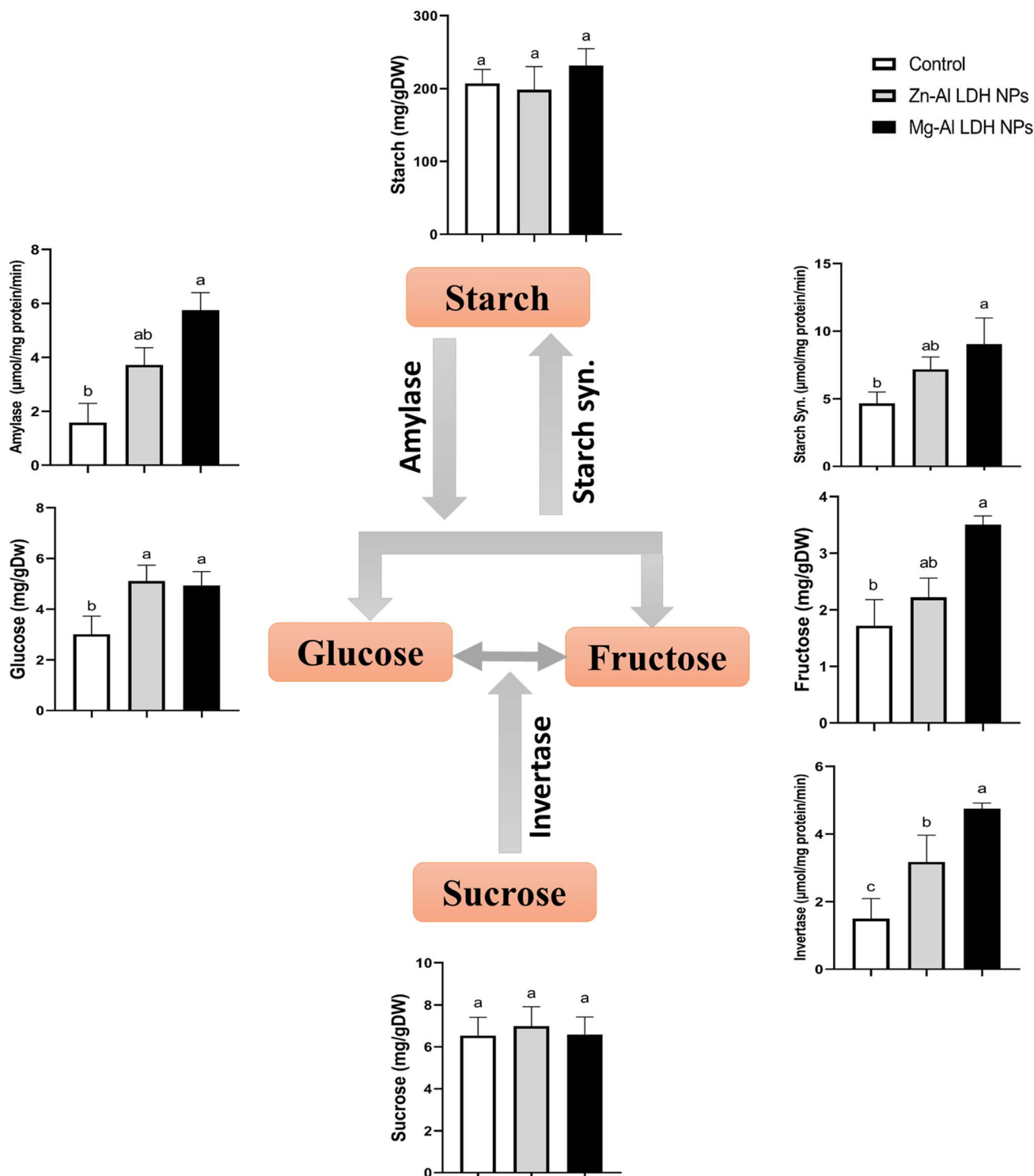


Fig. 1 The changes in the contents of soluble and non-soluble sugars in geranium shoots treated with Zn-Al LDH and Mg-Al LDH NPs. Vertical bars represented standard error (\pm SE). Different letters denoting significant changes between treatments are displayed above the bars ($P \leq 0.05$).

application caused a significant increase in invertase by 216% compared to the control. These increases were parallel with the non-significant inhibition of sucrose (4%) and accumulation of glucose and fructose by 62% and 105% respectively. This was also matched with non-significant increases in starch compared to the control.

3.5. Tri carboxylic acid contents (TCA)

The study measured the concentrations of six TCA – oxalate, malate, succinate, citrate, lactate, and *trans*-aconitic acids in geranium shoots treated with Zn-Al LDH and Mg-Al LDH NPs. The findings demonstrated that in contrast to the control



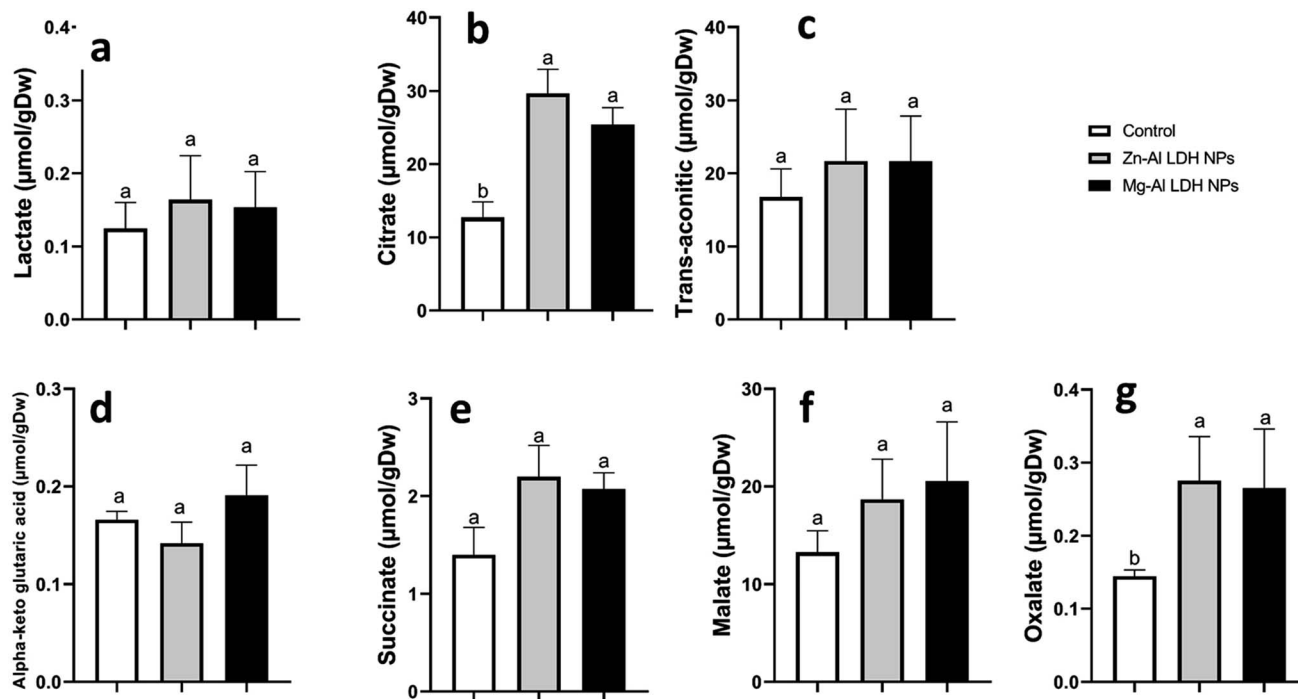


Fig. 2 The changes in the organic acids contents in geranium plant shoots treated with Zn-Al LDH and Mg-Al LDH NPs. Vertical bars represented standard error (\pm SE). Different letters denoting significant changes between treatments are displayed above the bars ($P \leq 0.05$).

group, the application of Zn-Al LDH and Mg-Al LDH NPs increased citrate levels by 133% and 100%, respectively, and oxalate by 89% and 82%, respectively. The levels of malate, succinate, lactate, and trans-aconitic were not significantly affected by the treatment with either Zn-Al LDH or Mg-Al LDH NPs Fig. 2.

3.6. Total protein and amino acids content

The amount of total protein and amino acids, including glycine, valine, phenylalanine, tyrosine, leucine, lysine, histidine, alanine, isoleucine, methionine, threonine, serine, aspartate, cystine, and asparagine, were measured in geranium shoots treated with Zn-Al LDH and Mg-Al LDH NPs (Fig. 3). Compared to the control, the application of Zn-Al LDH and Mg-Al LDH NPs had non-significant effects on the levels of both protein and amino acids, except for glycine, valine, phenylalanine, and tyrosine, which increased significantly in the case of Zn-Al LDH NPs by 66%, 127%, 101%, and 66%, respectively. On the other hand, treatment with Mg-Al LDH NPs resulted in significant increases in the amount of aspartate and tyrosine by 151% and 60%, respectively.

3.7. Proline metabolism

In this study, we examined the metabolites and important enzymes involved in the production of proline in geranium shoots *via* the glutamate and ornithine pathways (Fig. 4 and 5). The data showed that Mg-Al LDH NP increased the proline level by 170%, which correlated with the upregulation of both the ornithine (Fig. 5) and glutamine (Fig. 4) pathways. When

considering the ornithine pathway, comparing Mg-Al LDH NP to the control, there was not a significant difference in the levels of arginine and ornithine (Fig. 5). This finding was consistent with the upregulation of arginase by 276% and OAT by 99%. As for the glutamate pathway, Mg-Al LDH NP had a non-significant effect on α -ketoglutarate, glutamine, and glutamate. These results were associated with the activation of GOGAT (89%), GS (89%), P5CS (94%), and P5CR (121%) in contrast to the control group (Fig. 4).

3.8. Secondary metabolites

3.8.1 Tocopherols. In this study, we analyzed the secondary metabolites such as alpha-tocopherol, beta-tocopherol, gamma-tocopherol, and total tocopherol in geranium shoots (Fig. 6). The data indicated that Zn-Al LDH NP increased alpha-tocopherol by 7%, beta-tocopherol by 33%, gamma-tocopherol by 140%, and total tocopherol by 25%. However, there is no significant increase in alpha-tocopherol. Mg-Al LDH NPs increased alpha-tocopherol by 32%, beta-tocopherol by 53%, gamma-tocopherol by 112%, and total tocopherol by 45% compared to the control.

3.8.2 Phenolic content. In this investigation, the phenolic content of geranium shoots was analyzed Fig. 7. The data indicated that Zn-Al LDH NP increased rosmarinic acid by 990% compared to the control. Additionally, Mg-Al LDH NPs increased gallic acid by 103%, *p*-coumaric acid by 427%, and chicoric acid by 69% in contrast to the control group.

3.8.3 Flavonoid content. In this investigation, the flavonoid content of geranium shoots was examined Fig. 8. The data indicated that the content of flavonoids is not significantly

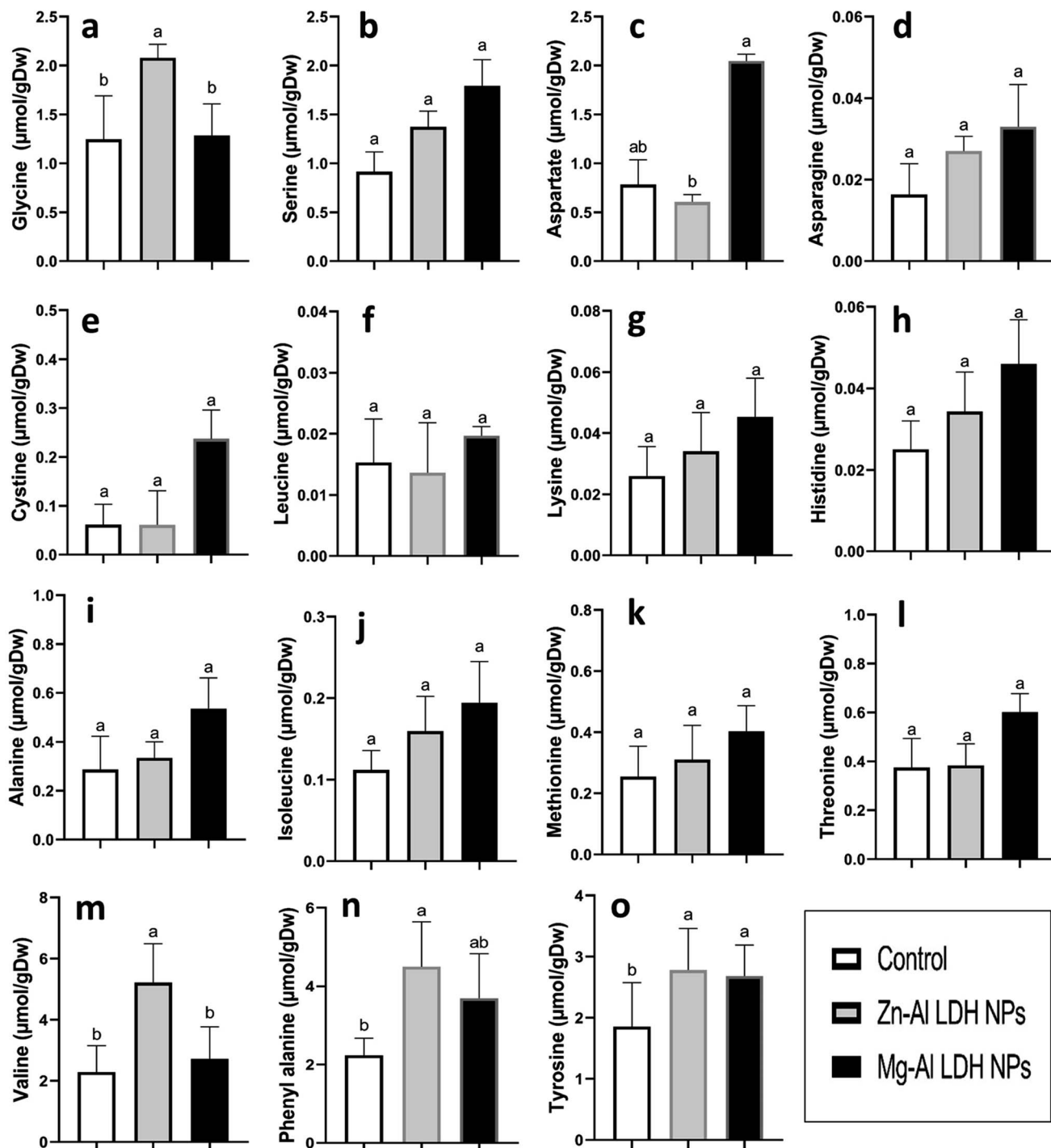


Fig. 3 The changes in amino acid contents in geranium shoots treated with Zn-Al LDH and Mg-Al LDH NPs. Vertical bars represented standard error (\pm SE). Different letters denoting significant changes between treatments are displayed above the bars ($P \leq 0.05$).

affected by Zn-Al LDH or Mg-Al LDH NPs, except in the case of Mg-Al LDH NP causing a 134% increase in kaempferol content compared to the control.

3.9. Principal component analysis (PCA)

To test the specific responses of shoots of geranium plant shoots plants to Zn-Al LDH and Mg-Al LDH NPs, we performed

PCA with growth, minerals, total chlorophyll, primary and secondary metabolites, and their related metabolic enzymes activate data set. The PCA embodied uniform growth, metabolites, and enzyme parameters along with PC1 and PC2 which declared 54% and 21% of the data variability, respectively (Fig. 9). PC1 separated the measured parameters based on LDH NP treatment (control vs. Zn-Al LDH and Mg-Al LDH NPs),



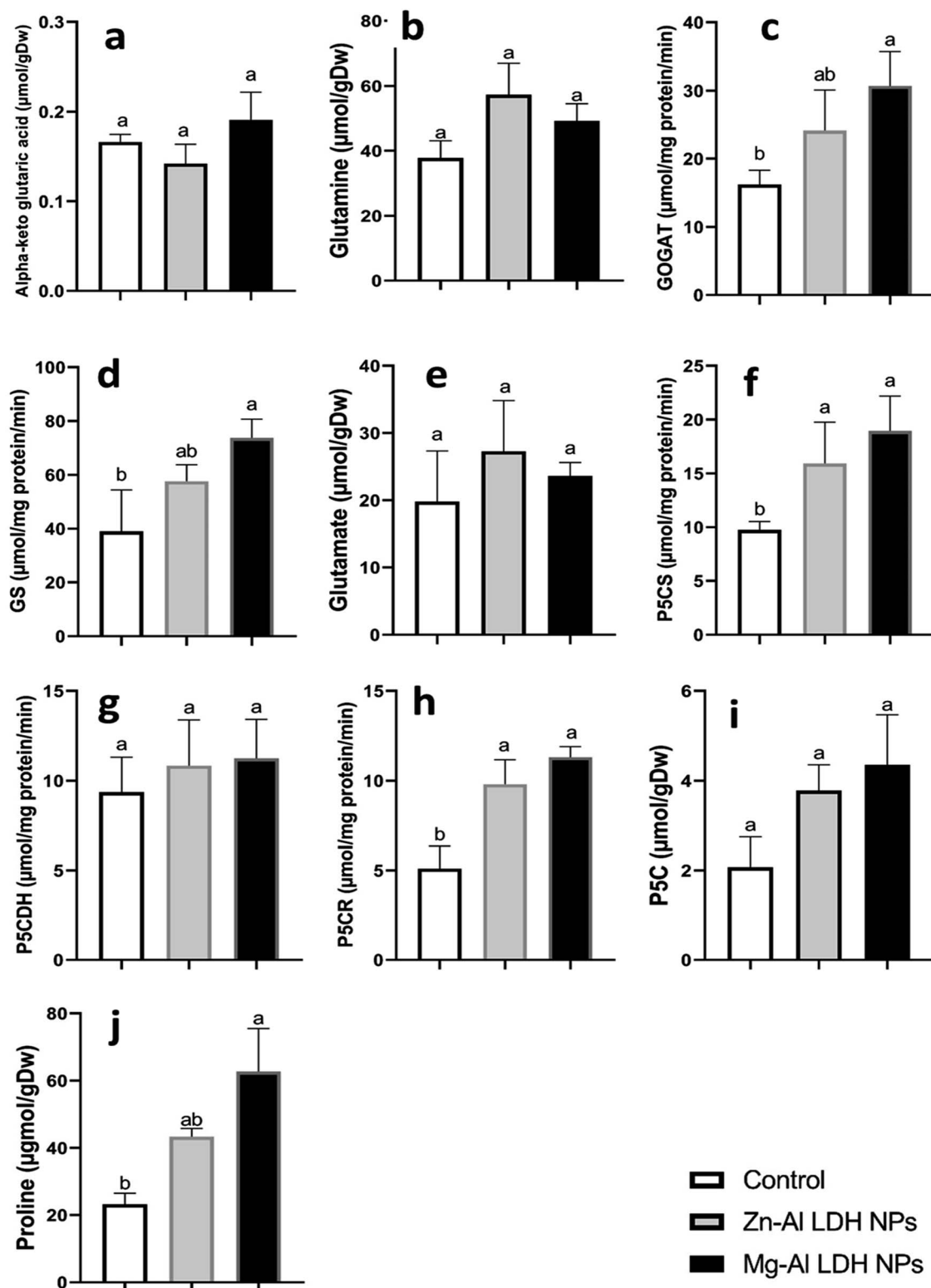


Fig. 4 The changes in glutamate pathway, a part of proline metabolism, in geranium shoots treated with Zn-Al LDH and Mg-Al LDH NPs. Vertical bars represented standard error (\pm SE). Different letters denoting significant changes between treatments are displayed above the bars ($P \leq 0.05$).

whereas the Zn-Al LDH vs. Mg-Al LDH NPs specific responses were separated along PC2. For LDH NP treatment, PC1 showed that these LDH NPs induced upregulation in all measured

parameters. PC2 showed that Mg-Al LDH NPs increased amino acid accumulation, however, major fatty acids and organic acids were more responsive to Zn-Al LDH NP treatment.

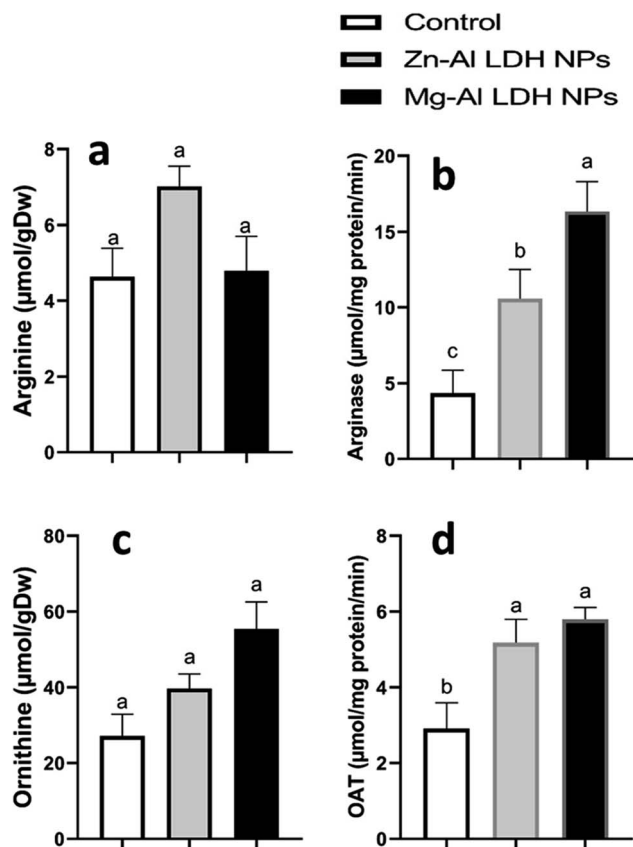


Fig. 5 The changes in amino acids and enzyme activities involved in the ornithine pathway, a part of proline metabolism, in geranium plant shoots treated with Zn-Al LDH and Mg-Al LDH NPs. OAT is ornithine aminotransferase. Vertical bars represented standard error (\pm SE). Different letters denoting significant changes between treatments are displayed above the bars ($P \leq 0.05$).

4. Discussion

4.1. Zn and Mg LDH NPs improved the biomass accumulation in geranium plants

Fertilizers are chemical chemicals used in plant cultivation to increase yield and productivity. Nano fertilizers are fertilizers made from nano-sized materials that supply one or more types of nutrients needed for the cultivation of plants.⁵³ Nano fertilizers have several advantages, such as improving nutrient uptake efficiency, increasing plant assimilation, and decreasing the negative environmental effects of conventional chemical fertilizers.^{54,55} Mg and Zn fertilizers positively induce cell division and mineral absorption, resulting in increased plant growth.^{18,56} The current study was done to evaluate the role of Zn-Al LDH and Mg-Al LDH NPs in growth and metabolic profiles in geranium plants. The growth enhancement of plants due to MgO-NP treatment can be attributed to various mechanisms, including improved nutrient availability, enhanced nutrient uptake, better water absorption, and increased antioxidant activity.⁵⁷ The impact of both LDH NPs on Zn and Mg accumulation was investigated by measuring the Zn and Mg content in the shoots of geranium seedlings (Table 1). This increase in Zn and Mg accumulation was linked to a significant

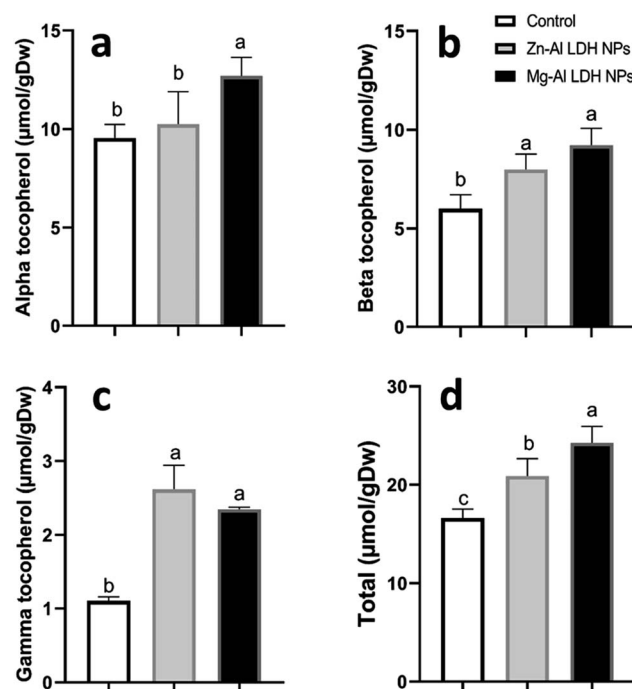


Fig. 6 The changes in tocopherol levels (alpha-tocopherol, beta-tocopherol, gamma-tocopherol, and total tocopherol) in geranium plant shoots treated with Zn-Al LDH and Mg-Al LDH NPs. Vertical bars represented standard error (\pm SE). Different letters denoting significant changes between treatments are displayed above the bars ($P \leq 0.05$).

rise in the biomass of treated geranium plants. Similarly, it was observed that Mg and Zn nutrients enhance growth parameters in mung bean plants.⁵⁶ Thus, our findings highlight the vital role LDH NPs play in enhancing photosynthesis.

4.2. Zn and Mg LDH NPs induced bioactive primary metabolites accumulation in geranium plants

NPs can improve the metabolism of carbon and nitrogen, which is connected to stimulated photosynthesis and enhances the growth and development of plants.⁵⁸ The metabolism of nitrogen and carbon are closely related activities.²⁵ Our study shows that utilizing Zn-Al LDH and Mg-Al LDH NPs increased photosynthetic pigments (Table 1). Numerous studies found similar improvements in photosynthetic pigments. For example, spraying foliar ZnO NPs on coffee plants improved photosynthesis and biomass growth.⁵⁹ NPs boosted the activity of major photosynthetic enzymes such as Rubisco, PEP carboxylase, and carbonic anhydrase.⁶⁰ This increase in enzyme activity, along with increased chlorophyll content, resulted in higher photosynthetic rates.⁶¹ Furthermore, NPs had a dual effect, lowering ROS generation while speeding up the electron transport chain in chloroplasts; these pathways lead to increased CO₂ fixation and photosynthetic performance.⁶²

A C-skeleton and an energy supply are provided by carbohydrate biosynthesis during photosynthesis for several plant functions, such as N absorption and inorganic N fixing.⁶³ It's important to note that C and N assimilate as sugars and amino acids serve as osmotic regulators and energy sources.⁶⁴ Because



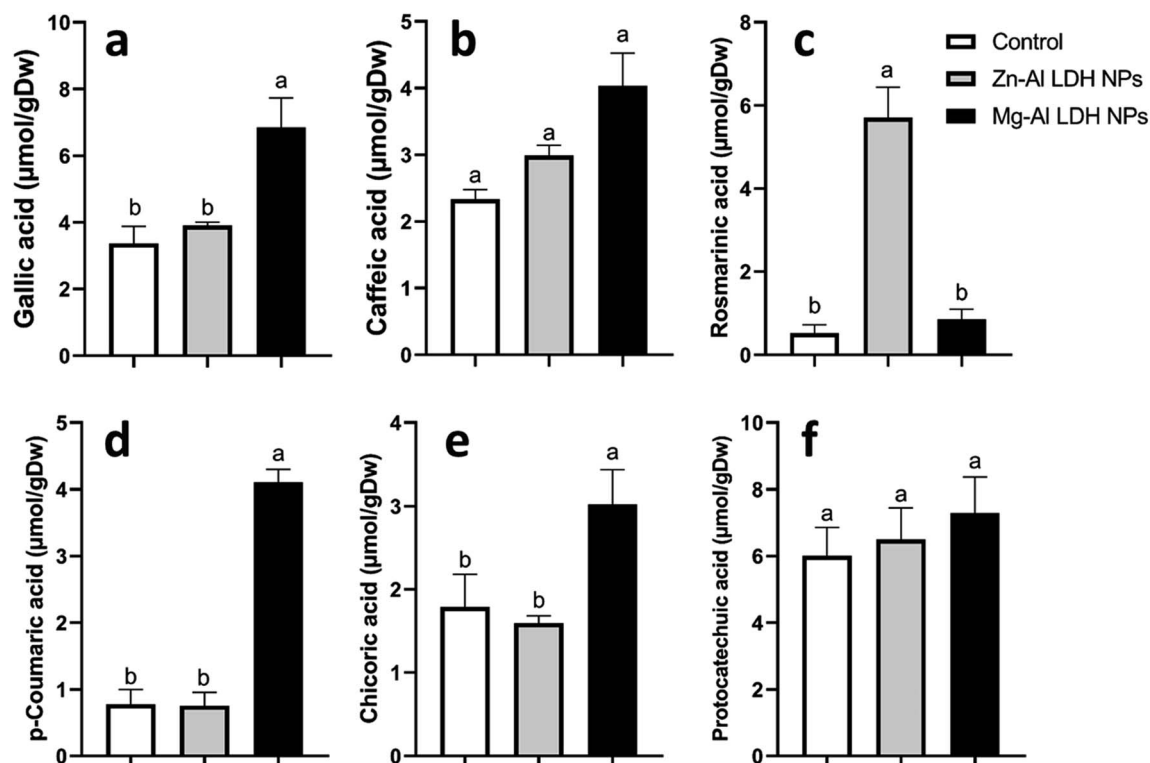


Fig. 7 The changes in phenolics content in geranium plant shoots treated with Zn-Al LDH and Mg-Al LDH NPs. Vertical bars represented standard error (\pm SE). Different letters denoting significant changes between treatments are displayed above the bars ($P \leq 0.05$).

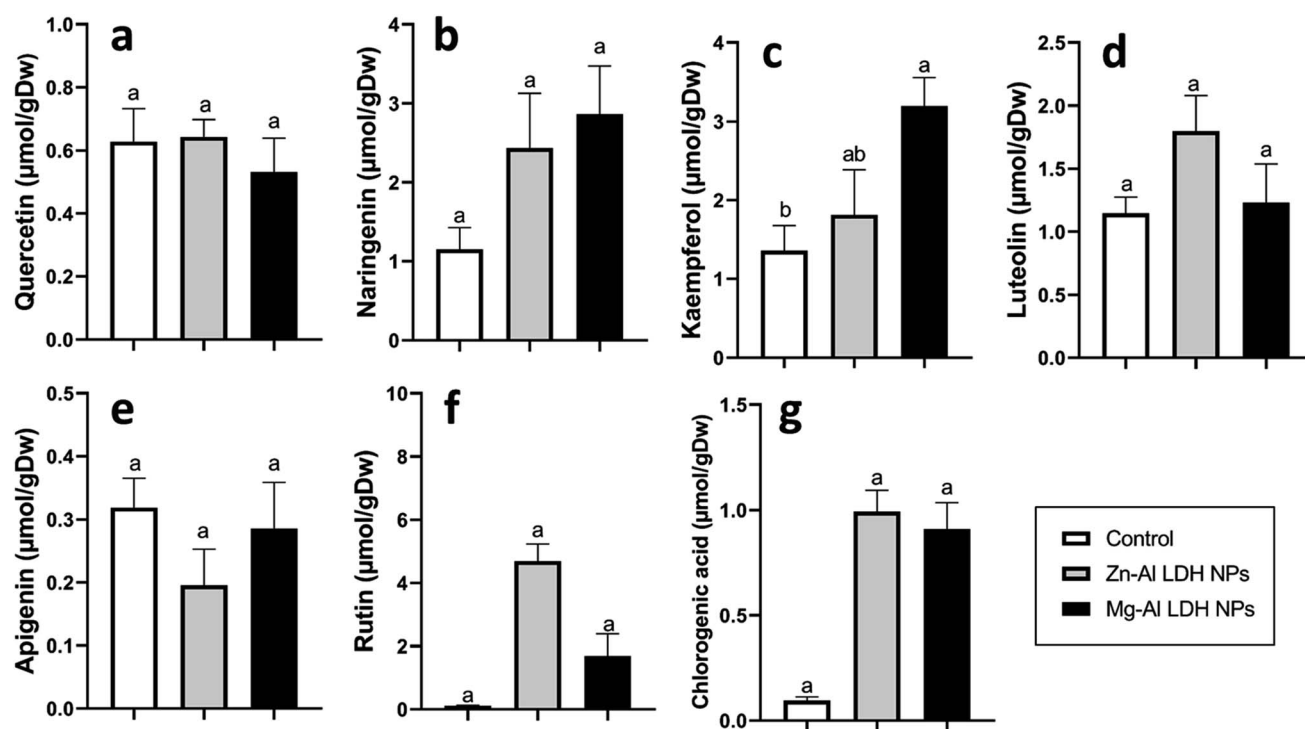
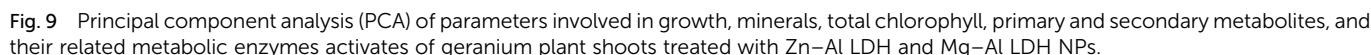


Fig. 8 The changes in flavonoid content in geranium plant shoots treated with Zn-Al LDH and Mg-Al LDH NPs. Vertical bars represented standard error (\pm SE). Different letters denoting significant changes between treatments are displayed above the bars ($P \leq 0.05$).



carbon metabolism.⁷⁰ Organic acids serve as the building blocks of plant metabolism.⁷¹ Plants have a vast array of metabolites, comprising organic acids like citric, malic, succinic, fumaric, and oxalic acids, that serve vital roles in plant metabolism and are engaged in critical processes such as the Krebs cycle.⁷² Malic acid is also involved in respiration and photosynthesis.⁷³ TCA organic acids are regarded as the connection between carbon and nitrogen metabolism. They are formed by the respiratory breakdown of carbohydrates and serve as the carbon skeleton needed for nitrogen assimilation and amino acid synthesis.⁷⁴ In line with our results, LDH NPs had non-significant effects on the levels of TCA acids levels (Fig. 2). This is related to the consumption of organic acids to synthesize amino acids. In the instance of Zn-Al, LDH NP had considerable effects on amino acid levels like tyrosine, phenylalanine, valine, and glycine (Fig. 3).

Essential amino acids have critical roles in increasing plant bioactivity by participating in many metabolic pathways that promote growth, stress tolerance, and overall health.⁷⁵ Amino acids are essential not only as protein building blocks but also as precursors for bioactive compounds that regulate physiological and biochemical processes. Glycine and serine play crucial roles in maintaining photorespiratory fluxes and providing carbon and nitrogen for metabolism in response to environmental changes in nature.⁷⁶ Glutamate, glutamine, aspartate, and asparagine are the principal products of nitrogen absorption, therefore pools are enormous, particularly in light.^{77,78} Amino acids like phenylalanine and tyrosine are precursors for flavonoid molecules, which play an important role in plant defense mechanisms.⁷⁹ Tocopherols, also known as vitamin E, are plant-derived natural products derived from tyrosine.⁸⁰ In addition to the accumulation of the bioactive and nutritive essential amino acids, proline is an amino acid known for its conformational rigidity and is vital for primary metabolism.²⁷ In many plants, proline accumulation supports the plant's defense mechanisms.⁸¹ Another proposed function of proline is the storage and transfer of energy.^{26–28} We observed an increase in proline in the instance of Mg–Al LDH NP-treated plants. This matched with the activation of GOGAT, GS, P5CS, and P5CR compared to the control.⁴⁴ Proline is synthesized using the glutamate and ornithine routes.⁸² Our data demonstrate that in geranium, both the glutamate and ornithine pathways (P5CS, P5CR, and OAT) are equally active under LDH NPs (Fig. 4 and 5). Previous studies have shown that ZnO-NPs lead to increased proline accumulation in tomato plants⁸³ and SiO₂-NPs have a similar effect on squash.⁸⁴

4.3. Zn and Mg LDH NPs improved the redox status of geranium plants

Increased amounts of primary metabolites, such as sugars and amino acids can serve as precursors for secondary metabolite synthesis. In this context, induced primary metabolism can influence regulatory mechanisms that control secondary metabolic pathways, further enhancing their production.⁸⁵ In line with our results, there was a rise in antioxidants, like tocopherols, phenolic, and flavonoid levels (Fig. 6–8). These metabolites are typically present in low concentrations and play a crucial role in all living organisms.³¹ Recently, there has been an increasing interest in these compounds due to their practical applications in nutrition, medicine, and cosmetics, as well as their undeniable role in plant stress physiology.³¹ These compounds, such as phenolic compounds, flavonoids, ascorbic acid, and vitamin E, help in scavenging harmful free radicals.⁸⁶ This suggests that the treated plants could reduce membrane lipid peroxidation by scavenging reactive oxygen species (ROS) and thus maintaining cellular structure.⁸⁷

Plants contain α -tocopherol, a key vitamin E component required for medical uses and human nourishment.⁸⁸ Tocopherols are powerful lipid-soluble antioxidants that protect cellular membranes from oxidative damage by scavenging lipid peroxyl radicals.⁸⁹ Tocopherols protect the thylakoid membranes in chloroplasts from oxidative damage, thus

preserving the photosynthetic machinery. For instance, α -tocopherol is found in high concentrations in chloroplasts, where it helps protect photosystem II (PSII) from oxidative stress caused by excess light.⁹⁰ Phenolic compounds and flavonoids act as antioxidants and have nutritional and medicinal properties. Bioactive compounds like phenolic acids are nutritional elements that are beneficial to human health and are found in small quantities in foods.⁹¹ Mg–Al LDH NPs increase the level of gallic acid, *p*-coumaric, and chicoric acid. Gallic acid has medicinal properties such as anti-fungal activity.⁹² *P*-coumaric is a good antioxidant and also exhibits strong antimicrobial properties.⁹³ Chicoric acid has been shown to have potential antioxidant, anti-inflammatory, antiviral, and immune-stimulating properties.⁹⁴ Zn–Al LDH NPs increase the levels of rosmarinic acid (Fig. 7). Similarly, lower concentrations of silver nanoparticles (SNPs) increased phenolic compounds, such as rosmarinic acid, in sage plants.⁹⁵ Flavonoids, an important class of natural antioxidants, play a significant role in removing free radicals⁹⁶ and have medicinal properties as antiviral, anti-inflammatory, anti-cancer, and anti-diabetic.⁹⁷ Our results indicate a positive effect of Mg–Al LDH NPs on kaempferol (Fig. 8). Similarly, other findings suggest that the application of ZnO or Fe₃O₄ NPs causes the highest concentration of flavonoids, specifically kaempferol, in potatoes.⁹⁸ TiO₂ and SiO₂ NPs led to increased production of α -tocopherol in argan.⁸⁸ Stevia callus tissue treated with 100 mg L^{−1} of ZnO NPs showed the highest levels of total flavonoid content, total phenolic content, and total antioxidant capacity.⁹⁹ NPs of CuO and ZnO increased the content of phenolic compounds in licorice seedlings.¹⁰⁰ MgO and Fe₂O₃ NPs had a significant effect on flavonoid levels in roselle.¹⁰¹ *Nigella arvensis* treated with TiO₂, Al₂O₃, and NiO NPs led to increased production of total flavonoids.¹⁰²

5. Conclusion

Based on the findings of this study, we can conclude that both LDH NPs significantly enhanced the growth and photosynthetic pigment and metabolic profiles in geranium plants.

Data availability

All data are presented in this article, and raw data is available upon request from the corresponding author.

Conflicts of interest

All authors declare that they have no competing interests.

Acknowledgements

The authors extend their appreciation to the researchers supporting project number (RSPD2024R931) at King Saud University, Riyadh, Saudi Arabia.



References

- 1 Y. Khan, H. Sadia, S. Zeeshan, A. Shah, M. N. Khan, A. A. Shah, N. Ullah, M. F. Ullah, H. Bibi, O. T. Bafakeeh, N. Ben Khedher, S. M. Eldin, B. M. Fadhl and M. I. Khan, *Catalysts*, 2022, **12**, 1386.
- 2 L. R. Khot, S. Sankaran, J. M. Maja, R. Ehsani and E. W. Schuster, *Crop Prot.*, 2012, **35**, 64–70.
- 3 A. Singha Roy, S. Kesavan Pillai and S. S. Ray, *ACS Omega*, 2022, **7**, 20428–20440.
- 4 A. Geremew, L. Carson, S. Woldesenbet, H. Wang, S. Reeves, N. Brooks, P. Saganti, A. Weerasooriya and E. Peace, *Front. Plant Sci.*, 2023, **14**, 1–16.
- 5 C.-H. Lin, H.-L. Chu, W.-S. Hwang, M.-C. Wang and H.-H. Ko, *AIP Adv.*, 2017, **7**(12), 125005.
- 6 X. Li, L. Wang, B. Chen, Y. Xu, H. Wang, F. Jin, Z. Shen and D. Hou, *Appl. Clay Sci.*, 2024, **249**, 107262.
- 7 A. Singha Roy, S. Kesavan Pillai and S. S. Ray, *ACS Omega*, 2023, **8**, 8427–8440.
- 8 V. K. Ameena Shirin, R. Sankar, A. P. Johnson, H. V. Gangadharappa and K. Pramod, *J. Controlled Release*, 2021, **330**, 398–426.
- 9 R. Salinas-Jiménez, G. Vera, M. Tobar, J. Moscote, G. Acha, A. Herrera-Vásquez, D. Rojas-Rivera, E. A. Vidal, A. M. Almeida and M. Ahumada, *Environ. Sci.: Nano*, 2024, **11**, 2249–2261.
- 10 M. Hamzah Saleem, K. Usman, M. Rizwan, H. Al Jabri and M. Alsafran, *Front. Plant Sci.*, 2022, **13**, 1033092.
- 11 M. U. Hassan, M. Aamer, M. U. Chattha, T. Haiying, B. Shahzad, L. Barbanti, M. Nawaz, A. Rasheed, A. Afzal and Y. Liu, *Agriculture*, 2020, **10**(9), 396.
- 12 A. Singha Roy, S. Kesavan Pillai and S. S. Ray, *ACS Omega*, 2022, **7**, 20428–20440.
- 13 J. Kameliya, A. Verma, P. Dutta, C. Arora, S. Vyas and R. S. Varma, *Inorganics*, 2023, **11**(3), 121.
- 14 J. Hong, C. Wang, D. C. Wagner, J. L. Gardea-Torresdey, F. He and C. M. Rico, *Environ. Sci.: Nano*, 2021, **8**, 1196–1210.
- 15 A. Babajani, A. Iranbakhsh, Z. Oraghi Ardebili and B. Eslami, *Environ. Sci. Pollut. Res.*, 2019, **26**, 24430–24444.
- 16 M. Faizan, J. A. Bhat, C. Chen, M. N. Alyemeni, L. Wijaya, P. Ahmad and F. Yu, *Plant Physiol. Biochem.*, 2021, **161**, 122–130.
- 17 N. Pandey, *Plant Nutrients and Abiotic Stress Tolerance*, 2018, pp. 51–93.
- 18 A. Abbasifar, F. Shahrabadi and B. ValizadehKaji, *J. Plant Nutr.*, 2020, **43**, 1104–1118.
- 19 P. Venkatachalam, N. Priyanka, K. Manikandan, I. Ganeshbabu, P. Indiraarulsevi, N. Geetha, K. Muralikrishna, R. C. Bhattacharya, M. Tiwari and N. Sharma, *Plant Physiol. Biochem.*, 2017, **110**, 118–127.
- 20 A. Hussain, S. Ali, M. Rizwan, M. Z. ur Rehman, M. R. Javed, M. Imran, S. A. S. Chatha and R. Nazir, *Environ. Pollut.*, 2018, **242**, 1518–1526.
- 21 A. Srivastav, D. Ganjewala, R. K. Singhal, V. D. Rajput, T. Minkina, M. Voloshina, S. Srivastava and M. Shrivastava, *Plants*, 2021, **10**, 2556.
- 22 D. Kanjana, *J. Plant Nutr.*, 2020, **43**, 3035–3049.
- 23 L. Cai, M. Liu, Z. Liu, H. Yang, X. Sun, J. Chen, S. Xiang and W. Ding, *Molecules*, 2018, **23**, 3375.
- 24 H. Abdelgawad, V. Avramova, G. Baggerman, G. Van Raemdonck, D. Valkenburg, X. Van Ostade, Y. Guisez, E. Prinsen, H. Asard and W. Van den Ende, *Plant, Cell Environ.*, 2020, **43**, 2254–2271.
- 25 H. Abdelgawad, Y. M. Hassan, M. O. Alotaibi, A. E. Mohammed and A. M. Saleh, *Sci. Total Environ.*, 2020, **749**, 142356.
- 26 E. Ábrahám, G. Rigó, G. Székely, R. Nagy, C. Koncz and L. Szabados, *Plant Mol. Biol.*, 2003, **51**, 363–372.
- 27 L. Szabados and A. Savouré, *Trends Plant Sci.*, 2010, **15**, 89–97.
- 28 P. E. Verslues and S. Sharma, *Arabidopsis Book/American Society of Plant Biologists*, 2010.
- 29 A. El Moukhtari, C. Cabassa-Hourton, M. Farissi and A. Savouré, *Front. Plant Sci.*, 2020, **11**, 553924.
- 30 S. de J. Rivero-Montejo, M. Vargas-Hernandez and I. Torres-Pacheco, *Agriculture*, 2021, **11**, 134.
- 31 A. Bartwal, R. Mall, P. Lohani, S. K. Guru and S. Arora, *J. Plant Growth Regul.*, 2013, **32**, 216–232.
- 32 K. M. Bester, W. W. Focke and F. J. W. J. Labuschagné, *AIP Conf. Proc.*, 2019, **2055**, 050009.
- 33 F. Mohamed, N. Bhnsawy and M. Shaban, *Sci. Rep.*, 2021, **11**, 1–14.
- 34 F. Mohamed, M. R. Abukhadra and M. Shaban, *Sci. Total Environ.*, 2018, **640–641**, 352–363.
- 35 J. Xie, K. Lee, H. Park, H. Jung and J.-M. Oh, *Nanomaterials*, 2023, **13**, 567.
- 36 H. K. Lichtenthaler, C. Buschmann and M. Knapp, *Photosynthetica*, 2005, **43**, 379–393.
- 37 A. R. M. Albakaa, D. S. M. Ameen, N. K. Abed, Z. A. Jabbar and L. A. Musaa, *J. Phys.: Conf. Ser.*, 2021, **1853**(1), 012018.
- 38 S. Al Jaouni, A. M. Saleh, M. A. M. Wadaan, W. N. Hozzein, S. Selim and H. Abdelgawad, *J. Plant Physiol.*, 2018, **224**, 121–131.
- 39 P. S. Kerr, T. W. Ruffy Jr. and S. C. Huber, *Plant Physiol.*, 1985, **77**, 275–280.
- 40 A. Nishi, Y. Nakamura, N. Tanaka and H. Satoh, *Plant Physiol.*, 2001, **127**, 459–472.
- 41 M. Madany and R. Khalil, *Egypt. J. Exp. Biol.*, 2017, **13**, 119–133.
- 42 M. S. M. Mohamed, H. M. Mostafa, S. H. Mohamed, S. I. Abd El-Moez and Z. Kamel, *Microb. Drug Resist.*, 2020, **26**, 1410–1420.
- 43 A. K. Sinha, T. Giblen, H. Abdelgawad, M. De Rop, H. Asard, R. Blust and G. De Boeck, *Aquat. Toxicol.*, 2013, **130**, 86–96.
- 44 H. Abdelgawad, D. De Vos, G. Zinta, M. A. Domagalska, G. T. S. Beemster and H. Asard, *New Phytol.*, 2015, **208**, 354–369.
- 45 O. H. Lowry, N. J. Rosebrough, A. L. Farr and R. J. Randall, *J. Biol. Chem.*, 1951, **193**, 265–275.
- 46 S. Lutts, V. Majerus and J. Kinet, *Physiol. Plant.*, 1999, **105**, 450–458.
- 47 G. Forlani, M. Bertazzini, M. Zarattini and D. Funck, *Front. Plant Sci.*, 2015, **6**, 150038.



- 48 S. A. Robinson, A. P. Slade, G. G. Fox, R. Phillips, R. G. Ratcliffe and G. R. Stewart, *Plant Physiol.*, 1991, **95**, 509–516.
- 49 S. J. Temple, S. Kunjibettu, D. Roche and C. Sengupta-Gopalan, *Plant Physiol.*, 1996, **112**, 1723–1733.
- 50 C. Charest and C. Ton Phan, *Physiol. Plant.*, 1990, **80**, 159–168.
- 51 H. Chen, B. C. McCaig, M. Melotto, S. Y. He and G. A. Howe, *J. Biol. Chem.*, 2004, **279**, 45998–46007.
- 52 N. H. Gomaa and H. R. AbdElgawad, *Span. J. Agric. Res.*, 2012, **10**, 492–501.
- 53 C. Dissanayake and R. Chandrajith, *J. Natl. Sci. Found. Sri Lanka*, 2009, **37**, 153–165.
- 54 J. S. Duhan, R. Kumar, N. Kumar, P. Kaur, K. Nehra and S. Duhan, *Biotechnol. Rep.*, 2017, **15**, 11–23.
- 55 R. Liu and R. Lal, *Sci. Total Environ.*, 2015, **514**, 131–139.
- 56 A. T. Thalooth, M. M. Tawfik and H. M. Mohamed, *World J. Agric. Sci.*, 2006, **2**, 37–46.
- 57 M. A.-A. Amin, A. M. Abu-Elsaoud, A. I. Nowwar, A. T. Abdelwahab, M. A. Awad, S. E.-D. Hassan, F. Boufahja, A. Fouda and A. Elkelish, *Green Process. Synth.*, 2024, **13**, 20230215.
- 58 S. S. Mukhopadhyay and N. Kaur, *Plant Nanotechnology: Principles and Practices*, 2016, pp. 329–348.
- 59 L. Rossi, L. N. Fedenia, H. Sharifan, X. Ma and L. Lombardini, *Plant Physiol. Biochem.*, 2019, **135**, 160–166.
- 60 A. Jahan, M. M. A. Khan, B. Ahmad, K. B. M. Ahmed, Y. Sadiq and M. Gulfishan, *Braz. J. Bot.*, 2023, **46**, 337–349.
- 61 S. Kataria, M. Jain, A. Rastogi, M. Živčák, M. Brestic, S. Liu and D. K. Tripathi, in *Nanomaterials in Plants, Algae and Microorganisms*, Elsevier, 2019, pp. 103–127.
- 62 T. C. Thounaojam, T. T. Meetei, Y. B. Devi, S. K. Panda and H. Upadhyaya, *Acta Physiol. Plant.*, 2021, **43**, 1–21.
- 63 M. D. Bolton, *Mol. Plant-Microbe Interact.*, 2009, **22**, 487–497.
- 64 I. I. Shabbaj, H. AbdElgawad, A. Tammar, W. A. Alsiary and M. M. Y. Madany, *Plant Physiol. Biochem.*, 2021, **166**, 1131–1141.
- 65 M. H. Rabie, M. E. Eleiwa, M. A. Aboseoud and K. M. Khalil, *J. King Abdulaziz Univ., Sci.*, 1992, **4**(1), 37–43.
- 66 R. Manivasagaperumal, S. Balamurugan, G. Thiagarajan and J. Sekar, *Curr. Bot.*, 2011, **2**, 11–15. 2011•core.ac.uk, <https://core.ac.uk/>.
- 67 R. N. Tharanathan, G. Muralikrishna, P. V. Salimath and M. R. R. Rao, *Proc. Plant Sci.*, 1987, **97**, 81–155.
- 68 H. AbdElgawad, A. E. Mohammed, J. R. van Dijk, G. T. S. Beemster, M. O. Alotaibi and A. M. Saleh, *Front. Plant Sci.*, 2023, **14**, 1–14.
- 69 D. L. Jones, *Plant Soil*, 1998, **205**, 25–44.
- 70 W. C. Plaxton and F. E. Podestá, *CRC Crit. Rev. Plant Sci.*, 2006, **25**, 159–198.
- 71 E. Hadavi and N. Ghazijahani, in *Biostimulants: Exploring Sources and Applications*, Springer, 2022, pp. 71–105.
- 72 T. A. Bennet-Clark, *New Phytol.*, 1933, 37–71.
- 73 C. Pereira, L. Barros, A. M. Carvalho and I. C. F. R. Ferreira, *Food Anal. Methods*, 2013, **6**, 1337–1344.
- 74 M. Lancien, P. Gadat and M. Hodges, *Plant Physiol.*, 2000, **123**, 817–824.
- 75 T. M. Hildebrandt, A. N. Nesi, W. L. Araújo and H.-P. Braun, *Mol. Plant*, 2015, **8**, 1563–1579.
- 76 X. Fu, L. M. Gregory, S. E. Weise and B. J. Walker, *Nat. Plants*, 2023, **9**, 169–178.
- 77 G. M. Coruzzi, *Arabidopsis Book/American Society of Plant Biologists*, 2003.
- 78 H.-M. Lam, K. Coschigano, C. Schultz, R. Melo-Oliveira, G. Tjaden, I. Oliveira, N. Ngai, M.-H. Hsieh and G. Coruzzi, *Plant Cell*, 1995, **7**, 887.
- 79 B. Heinemann and T. M. Hildebrandt, *J. Exp. Bot.*, 2021, **72**, 4634–4645.
- 80 C. A. Schenck and H. A. Maeda, *Phytochemistry*, 2018, **149**, 82–102.
- 81 M. Senthil-kumar and K. S. Mysore, *Plant, Cell Environ.*, 2012, **35**, 1329–1343.
- 82 M. M. F. Mansour and K. H. A. Salama, *Plant Ecophysiology and Adaptation under Climate Change: Mechanisms and Perspectives II: Mechanisms of Adaptation and Stress Amelioration*, 2020, pp. 357–397.
- 83 M. Faizan, A. Faraz, M. Yusuf, S. T. Khan and S. Hayat, *Photosynthetica*, 2018, **56**, 678–686.
- 84 M. H. Siddiqui, M. H. Al-Whaibi, M. Faisal and A. A. Al Sahli, *Environ. Toxicol. Chem.*, 2014, **33**, 2429–2437.
- 85 S. W. Drew and A. L. Demain, *Annu. Rev. Microbiol.*, 1977, **31**, 343–356.
- 86 D. M. Kasote, S. S. Katyare, M. V. Hegde and H. Bae, *Int. J. Biol. Sci.*, 2015, **11**, 982–991.
- 87 I. I. Shabbaj, M. M. Y. Madany, A. Tammar, M. A. Balkhyour and H. AbdElgawad, *Environ. Sci.: Nano*, 2021, **8**, 1960–1977.
- 88 G. A. Hegazi, W. M. Ibrahim, M. H. Hendawy, H. M. Salem and H. E. Ghareb, *Plant Arch.*, 2020, **20**, 2431–2437.
- 89 E. Niki, *Free Radical Biol. Med.*, 2014, **66**, 3–12.
- 90 S. Munné-Bosch and L. Alegre, *CRC Crit. Rev. Plant Sci.*, 2002, **21**, 31–57.
- 91 H. Boz, *Int. J. Food Sci. Technol.*, 2015, **50**, 2323–2328.
- 92 A. El-Nagar, A. A. Elzaawely, N. A. Taha and Y. Nehela, *Agronomy*, 2020, **10**, 1402.
- 93 P. S. Ferreira, F. D. Victorelli, B. Fonseca-Santos and M. Chorilli, *Crit. Rev. Anal. Chem.*, 2019, **49**, 21–31.
- 94 J. Lee and C. F. Scagel, *Food Chem.*, 2009, **115**, 650–656.
- 95 S. H. Moazzami Farida, R. Karamian and B. R. Albrechtsen, *Physiol. Plant.*, 2020, **170**, 415–432.
- 96 M. Modarresi, A. Chahardoli, N. Karimi and S. Chahardoli, *Heliyon*, 2020, **6**(6), e04265.
- 97 T. Wang, Q. Li and K. Bi, *Asian J. Pharm. Sci.*, 2018, **13**, 12–23.
- 98 A. R. Sallam, A. A. Mahdi and K. Y. Farroh, *Plant Cell Biotechnol. Mol. Biol.*, 2022, **23**, 1–16.
- 99 R. Javed, B. Yucesan, M. Zia and E. Gurel, *Sugar Technol.*, 2018, **20**, 194–201.
- 100 H. Oloumi, R. Soltaninejad and A. Baghizadeh, *Indian J. Plant Physiol.*, 2015, **20**, 157–161.
- 101 H. Kiapour, P. Moaveni, B. Sani, F. Rajabzadeh and H. Mozafari, *J. Med. Plants By-Prod.*, 2020, **9**, 19–31.
- 102 M. Modarresi, A. Chahardoli, N. Karimi and S. Chahardoli, *Heliyon*, 2020, **6**, e04265.

